SYNTHESIS, CHARACTERIZATION AND COMPUTATIONAL STUDIES OF PYRENE-BASED CHALCONE DERIVATIVES AND THEIR NONLINEAR OPTICAL PROPERTIES

SALEH KARAMA OBAID ALSAEE

UNIVERSITI SAINS MALAYSIA

2025

SYNTHESIS, CHARACTERIZATION AND COMPUTATIONAL STUDIES OF PYRENE-BASED CHALCONE DERIVATIVES AND THEIR NONLINEAR OPTICAL PROPERTIES

by

SALEH KARAMA OBAID ALSAEE

Thesis submitted in fulfilment of the requirements
for the degree of
Doctor of Philosophy

May 2025

ACKNOWLEDGEMENT

First and foremost, I express my deepest gratitude to Allah, whose grace and mercy granted me the strength, ability, and opportunity to complete this journey. Without His blessings, this achievement was impossible.

I would also like to extend my deepest gratitude to my supervisor, Prof. Dr. Abdul Razak Ibrahim and co-supervisor, Assoc. Prof. Dr. Suhana Arshad for their continuous and invaluable supervision, guidance, constructive guidance, insightful feedback, patience, and encouragement throughout my entire Ph.D. journey. Their suggestions have been instrumental in writing and completing this thesis.

My deepest thanks go to Dr. Mundzir Abdullah, Mohamad Aizat Abu Bakar, Dr. Dian Alwani, Dr. Wong Qin Aii, Dr. Muhamad Fikri Zaini, Ainizatul Husna Anizaim, Dr. Mohd Mustaqim Rosli, and Dr. Hemamalini Madhukar for their collaboration in experiments and data analysis. I am also grateful to my lab mates and staff, especially Nor Izzati Hashim, Nur Awanis Sirat, Elham Mazwd, Dr. Shawbo Abdulsamad Abubaker, Aliya, Farhana, Heng, Rines, Amin, Farah Diana Ramzi, Nur Aisyah Mohamad, and Hajar Wahida—for their constant assistance.

I dedicate this thesis to my parents, Karama Alsaee and Fatima Bin-Obidon; my wife, Zainb bin-Garmos; my grandmother, Zaianah; my children, Abdularahman, Rahaf, and Zulfa. Their support, patience, and prayers inspired me. I also thank my brother, Hassan, and all family members for caring for my family in my absence.

Lastly, I gratefully acknowledge Hadramout University, Sheikh Abdullah Bugshan, and the Hadhramout Foundation for Human Development for awarding me a Ph.D. scholarship. Without their financial support, this study would not have been possible.

TABLE OF CONTENTS

LIST OF TABLES

Page

LIST OF FIGURES

Page

LIST OF SYMBOLS

1A-1D	Halogen chalcone compounds group
2A-2E	Amine chalcone compounds group
3A-3D	Thiophene chalcone compounds group
4A-4D	Hydrocarbon chalcone compounds group
α	Linear polarizability
$\langle\alpha\rangle$	Dynamic linear polarizability
β	Dynamic first-order hyperpolarizability
β_{eff}	Effective nonlinear optical coefficient
γ	Dynamic second-order hyperpolarizability
c_g	Centroid
δ	Chemical shift
$\vec{E}$	Electromagnetic field
$E^{(2)}$	delocalization interactions energy
E_g	Energy gap
eV	Electron volt
μ	Dipole moment
μ_0	Permanent dipole moment
mL	Milliliter
mg	Milligram
mW	Milli Watt
nm	Nanometer
P	Induced polarization
$\pi \rightarrow \pi^*$	Electronic transition or hyperconjugative interaction from bonding π -orbital to antibonding π-orbital.

$\pi^* \rightarrow \pi^*$	Hyperconjugative interaction from antibonding π -orbital to antibonding π-orbital.
$n \rightarrow \pi^*$	Electronic transition or hyperconjugative interaction from bonding n -orbital to antibonding π-orbital.
$\sigma \rightarrow \sigma^*$	Hyperconjugative interaction from bonding sigma orbital to antibonding sigma orbital.
X	Halogen atom
$\chi^{(1,2,3)}$	Linear optical susceptibility, 2nd and 3rd order nonlinear susceptibility
ε_0	Permittivity of free space
6311G(d,p)	split-valence triple-zeta basis set with d,p type polarization functions
$\lambda_{\mathrm{Mo-K\alpha}}$	Wavelength of the X-ray in used SCXRD

LIST OF ABBREVIATIONS

A	Acceptor
ATR	Attenuated total reflectance
B3LYP	Becke's three-parameter with the Lee-Yang-Parr
CA	Close aperture
CAM	Coulomb-attenuating method
CAS	Chemical Abstracts Service
CCD	Charge-Coupled Device
CCDC	Cambridge Crystallographic Data Centre
$CDCl_3$	Deuterated chloroform
CIF	Crystallographic Information file
CW	Continuous wave
D	Donor or Debye
DFT	Density functional theory
DMSO	Dimethyl sulfoxide
DMSO-d6	Deuterated Dimethyl sulfoxide
EDG	Electron donating group
E_{HOMO}	Energy of HOMO level
E_{LUMO}	Energy of LUMO level
ESP	Electrostatic potential
esu	Electrostatic unit
EWG	Electron withdrawing group
FMO	Frontier molecular orbital
Fobs	Observed structure factor amplitudes
FTIR	Fourier transform infrared

GRD	Global reactivity descriptore
HOMO	Highest occupied molecular orbital
ICT	Intramolecular charge transfer
IEFPCM	Integral equation formalism polarizable continuum model
IR	Infrared
KDP	Potassium dihydrogen phosphate
LUMO	Lowest unoccupied molecular orbital
MEP	Molecular electrostatic potential
MeOH	Methanol
M.W	Molecular weight
n_2	Nonlinear refractive index
NaOH	Sodium Hydroxide
NBO	Natural bonding orbital
ND-filter	Neutral density filter
NIR	Near infrared
NLA	Nonlinear Absorption
NLO	Nonlinear optic
NLR	Nonlinear Refraction
nm	Nanometer
NMR	Nuclear magnetic resonance
OA	Open aperture
OL	Optical limiting
ORTEP	Oak Ridge Thermal Ellipsoid Plot
ppm	Parts per million
RSA	Reverse Saturable Absorption
SADABS	Siemens Area Detector Absorption Correction
SAINT	SAX Area-detector Integration (SAX-Siemens Analytical X-ray)

SCF	Self-Consistent Field
SCXRD	Single crystal X-ray diffraction
SFG	Sum-frequency generation
SHG	Second harmonic generation
SMART	Siemens Molecular Analysis Research Tools
SPR	Structure-property relationship
TICT	Twisted intramolecular charge transfer
TLC	Thin-Layer Chromatography
TLM	Thermal lens model
TMS	Tetramethylsilane
TPA	Two photon absorption
TD-DFT	Time dependent density functional theory
UV-Vis	Ultraviolet-visible
USM	Universiti Sains Malaysia
wR	Weighted Reliability Index

LIST OF APPENDICES

SINTESIS, PENCIRIAN DAN KAJIAN KOMPUTASI BAGI TERBITAN KALKON BERASASKAN PIRENA DAN SIFAT OPTIK TAK LINEAR

ABSTRAK

Sifat unik pirenil-kalkon (PChs) termasuk elektron π-delokalisasi yang kuat dan struktur yang boleh ditala, menawarkan potensi yang besar untuk teknologi optik termaju sebagai alternatif yang berpotensi, kos efektif dan pilihan mampan untuk fotonik optik tidak linear (NLO) berprestasi tinggi. Di sini, tujuh belas PChs baharu telah disintesis melalui kondensasi Claisen-Schmidt dan dikelaskan kepada empat kumpulan: kalkon halogen (1A-1D), kalkon amina (2A-2E), kalkon tiofena (3A-3D), dan kalkon hidrokarbon (4A-4D). Semua sebatian dihablurkan semula melalui kaedah penyejatan perlahan dan hanya sembilan sebatian membentuk hablur tunggal. Analisis pembelauan sinar-X hablur tunggal (SCXRD) dijalankan untuk mengkaji struktur kristalografi. Kajian spektroskopi sebatian dilakukan menggunakan teknik-teknik spektroskopi inframerah transformasi Fourier (FTIR), resonans magnetik nuklear (NMR), dan ultralembayung-nampak (UV-Vis) penyerapan. NLO dinilai menggunakan teknik imbasan-Z dan pengukuran had optik. Selain kajian eksperimen, kajian pengkomputeran merangkumi pengoptimuman struktur, pengiraan tenaga, orbital molekul frontier (FMO), potensi elektrostatik molekul (MEP), orbital ikatan semula jadi (NBO), frekuensi, dan pengiraan kekutuban dilakukan menggunakan teori fungsi ketumpatan (DFT) pada set asas B3LYP/6-311++G(d,p). Disamping itu, transisi elektronik berkaitan keadaan teruja dikaji menggunakan DFT sandaran-masa (TD-DFT) pada CAM-B3LYP/6-311++G(d,p). Keputusan SCXRD mendedahkan interaksi antara molekul yang pelbagai, termasuk C-H···O, C-H···X, C-H···π, dan π···π, yang menyusun molekul dalam konfigurasi kepala-ke-ekor, sisi-ke-muka, dan

muka-ke-muka. Analisis UV-Vis (secara eksperimen dan teori) menunjukkan penyerapan yang kuat dalam julat tampak dengan ketinggian antara 357-409 nm, dan spektrum menunjukkan transmisi penuh dalam julat tampak, penting untuk prestasi NLO yang tinggi. Peta MEP menekankan tapak elektrofilik dan nukleofilik di mana cas positif, neutral, dan negatif berada pada molekul, menekankan pengagihan cas dan haluan untuk pemindahan cas. Analisis NBO mendedahkan interaksi hiperkojugasi yang ketara seperti $\sigma \rightarrow \sigma^*$, $n \rightarrow \pi^*$, $\pi \rightarrow \pi^*$,$\pi^* \rightarrow \pi^*$, dengan nilai tinggi bagi tenaga interaksi delokalisasi $E^{(2)}$. Sebatian ini menunjukkan ciri kutub yang kuat dengan momen dwikutub (μ) dalam julat 2.1D hingga 8.9D, kebolehkutuban linear dinamik ($\langle\alpha\rangle$) antara 59 x10^{-24} esu hingga 125x10^{-24} esu, hiper-kebolehkutuban tertib pertama dinamik (β) dari 20.7 x10^{-30}esu hingga 601 x10^{-30}esu, dan hiper-kebolehkutuban tertib kedua dinamik (γ) dari 321 x10^{-36}esu hingga 4508 x10^{-36}esu. Keputusan ini menunjukkan kesan gantian terhadap ciri kutub molekul dalam julat yang luas. Pengukuran imbasan-Z tak menunjukkan kesan nyahfokus sendiri daripada profil pembiasan tak linear (NLR), dan penyerapan tepu songsang (RSA) daripada profil penyerapan tak linear (NLA). Disebabkan oleh elektron π-terdelokalisasi yang kuat dengan konfigurasi tolak-tarik yang kuat, kerentanan tertib ketiga untuk sebatian ini adalah dalam julat 0.42x10^{-5}esu hingga 2.34x10^{-5}esu. Tindak balas had optik untuk semua sebatian menunjukkan nilai had optik yang rendah dalam julat 491 mW hingga 1391 mW disebabkan oleh penggantian yang berbeza pada sebatian tersebut. Berdasarkan kajian ini, PChs adalah bahan berpotensi untuk peranti NLO dan penghad optik.

SYNTHESIS, CHARACTERIZATION AND COMPUTATIONAL STUDIES OF PYRENE-BASED CHALCONE DERIVATIVES AND THEIR NONLINEAR OPTICAL PROPERTIES

ABSTRACT

The unique properties of pyrenyl-chalcones (PChs) including strong π-delocalized electrons and a tuneable structure, offer significant potential for advanced optical technologies as a promising, cost-effective, and sustainable alternative for high-performance nonlinear optical (NLO) photonics. Herein seventeen novel PChs were synthesized through Claisen-Schmidt condensation and classified into four groups: halogens (1A-1D), amines (2A-2E), thiophene (3A-3D), and hydrocarbon (4A-4D) chalcones. All compounds were recrystalized via slow evaporation method and only nine compounds form single crystals. Single crystals X-ray diffraction (SCXRD) analysis was performed to investigate crystallographic structure. Spectroscopy studies of the compounds were performed using Fourier transform infrared (FTIR), nuclear magnetic resonance (NMR), and ultraviolet-visible (UV-Vis) absorption techniques. NLO properties were evaluated using the Z-scan technique and optical limiting measurements. Besides experimental investigation, computational studies including optimization structure, energy calculations, frontier molecular orbital (FMO), molecular electrostatic potential (MEP), natural bonding orbital (NBO), frequency, and polar calculations were utilized using density functional theory (DFT) at B3LYP/6-311++G(d,p) basis set. Additionally, electronic transition related to excited states were explored using time-dependent DFT (TD-DFT) at CAM-B3LYP/6-311++G(d,p). SCXRD results revealed diverse intermolecular interactions, including C-H···O, C-H···X, C-H··· π, and $\pi \ldots \pi$ which arranged the molecules in head-to-tail,

edge-to-face and face-to-face configurations. UV-Vis analysis (experimentally and computationally) showed strong absorption in the visible range with peaks between 357-409 nm, and the spectra indicated full transmittance in the visible range, crucial for strong NLO performance. MEP maps emphasized the electrophilic and nucleophilic sites where positive, neutral, and negative charges are on the molecule, highlighting charge distribution and pathways for charge transfer. NBO analysis revealed significant hyperconjugative interactions of $\sigma \rightarrow \sigma^*$, $n \rightarrow \pi^*$, $\pi \rightarrow \pi^*$, and $\pi^* \rightarrow \pi^*$, with high values of delocalization interactions energy $E^{(2)}$. The compounds exhibited strong polar properties with dipole moments(μ) ranging from 2.1D to 8.9D, dynamic linear polarizabilities ($\langle \boldsymbol{\alpha} \rangle$) from 59 x$10^{-24}$esu to 125x$10^{-24}$esu, dynamic first-order hyperpolarizability (β) from 20.7 x10^{-30}esu to 601 x10^{-30}esu, and dynamic second-order hyperpolarizabilities (γ) from 321 x10^{-36}esu to 4508 x10^{-36}esu. These results show the effect of the substituents on polar properties of the molecules within wide of range. Z-scan measurements revealed self-defocusing effects from nonlinear refraction (NLR) profiles, and reverse saturable absorption (RSA) from nonlinear absorption (NLA) profiles. Due to strong delocalized π-conjugated electrons with strong push-pull configuration, the third-order susceptibility ranged from 0.42x10^{-5} esu to 2.34x10^{-5}esu. Optical limiting responses for all compounds show low optical limiting values in the range of 491-1391 mW due to different compounds substituents. Based on this study, the PChs are promising materials for NLO devices and optical limiters.

CHAPTER 1

INTRODUCTION

1.1 Background

Nonlinear optical (NLO) analysis is a branch of optical research that studies the interaction of intense and coherent optical electromagnetic fields, within the range of atomic and inter-atomic fields, with the material molecules to generate new fields at different amplitudes, phases, and wavelengths [1]. The potential applications of NLO materials in optoelectronic fields, such as optical switching, optical limiting, optical computing, optical data storage, and telecommunications, have grabbed the interest of scientific community [2]–[4]. NLO materials with a higher NLO response enable to manipulate the frequency and phase of the incident light [5]. Consequently, the enormous optoelectronic applications of NLO materials have attracted material scientist to design reliable and stable structural configurations for high performance with fast nonlinearity response.

The study of molecular structures and their relationship with the desired optical properties has attracted many researchers in synthesizing new compounds and fabricating devices that exhibit the desired optical properties. Molecular structure-property relationships are directly related to many factors such as electronic structure, vibrational modes, intermolecular interactions, and intramolecular interactions [6].

For the past few decades, inorganic NLO materials were dominant in many different optical applications due to their high mechanical and high melting point [7]. However, their limitations in terms of low performance NLO, slow intrinsic response, and poor transmission have encouraged the development of novel organic NLO material configurations to overcome these limitations [7]. The conjugated structure organic materials, incorporating a push-pull system, offers superior promising NLO

properties compared to inorganic molecules, including lower dielectric constant, higher laser damage threshold, and grater design flexibility [8]–[10]. Additionally, the ease with which organic materials can be tuned by selecting appropriate substituents with suitable configuration makes them promising candidates for NLO applications in the photonic field.

1.1.1 Role of hyperpolarizability in NLO effectiveness

When a material is subjected to an intensive electromagnetic field ($\vec{E}$), the atoms or molecules within it experience polarization. This induced polarization (P) can be described by the following expression (1.1):

$$\mathrm{P} = \varepsilon_0\left[\chi^{(1)}\vec{E} + \chi^{(2)}\vec{E}\vec{E} + \chi^{(3)}\vec{E}\vec{E}\vec{E} + \cdots\right] \tag{1.1}$$

ε_0, $\chi^{(1)}$, $\chi^{(2)}$, and $\chi^{(3)}$ represent the permittivity of free space, linear optical susceptibility tensor of the medium, second order NLO susceptibility, and third order NLO susceptibility, respectively. These optical parameters rely on atomic structure of the material and frequency of $\vec{E}$. In addition, the NLO susceptibility terms are related to the molecular material level. At microscopic level, nonlinear dipole moment, μ, depends on the hyperpolarizability (β) and second hyperpolarizability (γ) and can be expressed in terms of polarizability coefficients as in the following equation:

$$\mu = \mu_0 + \alpha\vec{E} + \beta\,\vec{E}\vec{E} + \gamma\vec{E}\vec{E}\vec{E} + \cdots \tag{1.2}$$

In this equation, μ_0, α, are permanent dipole moment, and linear polarizability, respectively. β and γ are the first and second hyperpolarizability, respectively. Hyperpolarizability is a measure of nonlinear response of a molecule's electron cloud under an external applied electric field. The first hyperpolarizability β governs second-order NLO phenomena, such as second-harmonic generation (SHG), sum-frequency generation (SFG), and electro-optic modulation. Meanwhile, the second

hyperpolarizability (γ) is associated with third-order NLO effects, including third-harmonic generation (THG), two-photon absorption (TPA), and optical Kerr effect. β is related to the charge transfer of delocalized electrons from the donor to the acceptor part of the molecule , whereas the γ is determined by electronic polarization [11]. On molecular level, the applied electric optical field ($\vec{E}$) interact with binding forces leading to displace electrons positions from their equilibrium positions contributing in microscopic polarizability. The optical nonlinearity response for this microscopic polarizability in materials are related to various types of nonlinear effects, such as second harmonic generation (SHG), sum-frequency generation (SFG), third harmonic generation (THG), two photon absorption (TPA), optical Kerr effect, etc [12].

1.1.2 Third-order NLO for organic materials

Molecular engineering suggests that the organic materials exhibit stronger optical nonlinearity than inorganic materials. Organic materials show fast optical response time, high laser damage threshold, and easy to tune their molecular structure [13]–[17]. These advantages make them more suitable than inorganic materials as NLO materials. Organic materials exhibit a wide variety of tunable properties due to the ability of carbon atom to form stable hybridized bonds. In addition, carbon atoms can interact other atoms in terms of two type of bonding σ and π bonds. The σ-bond is formed by head-to-head coaxial overlapping between atomic orbitals [18] which is observed as an absorption peak in UV-region. On the other hand, the π-bond originates from delocalized electronic charges due to lateral overlap of atomic orbitals in which the absorption peak is shifted to larger wavelengths. The optical nonlinearity highly depends on the polarizability of delocalized π-electrons [19]. The third order NLO describes the phenomenon in which optical materials response related to the third power of the applied electric optical field ($\vec{E}$). The third-order NLO is characterized

via third-order susceptibility ($\chi^{(3)}$) which is related to the third-order hyperpolarizability in terms of induced dipole moment per unit volume.

1.2 Chalcones as NLO materials

Chalcones composite of two aromatic rings linked by an α,β unsaturated carbonyl system [20]. In chalcones structure, the chromophoric groups are separated by keto-vinyl chain which give this structure ability to enhance non-linear optical properties [21]. Chalcones and their derivatives have emerged as the NLO chromophores materials due to their high nonlinear optical response to the laser beam. The optical nonlinearity in this kind of materials originates from the delocalized nature of the π- electrons [22]. Moreover, the importance of the intramolecular charge transfer (ICT) has resulted in the designing of desired NLO molecules with different donor/acceptor groups. The structural analysis of the of some chalcone compounds show the continuous conjugation extends over the whole structure. From the structure point of view, the push-pull system which consists of electron donating groups (EDG) and electron withdrawing groups (EWG) coupled by π-conjugated bridge enhances the intramolecular charge transfer (ICT) of the molecule which directly improve the optical nonlinearity response of the compound. One of the important potential applications for organic NLO materials is their optical limiting (OL) effect, where the optical transmission of the material decreases as the laser intensity increases. The OL effect is dependent on the nonlinear absorption (NLA), and the factors that influence OL are the same as those that affect NLA [23], [24].

1.3 Structure-Property relationship (SPR) for NLO organic materials

Structure-property relationship (SPR) points to the corelation between the molecular structure of the material and its physical and chemical properties. In organic

NLO studies, the SPR investigates the relationship between the molecular structure and the NLO response. Hence molecular structure is related to the molecular geometry, electronic distribution, longitudinal of the conjugated pathway, presence and strength of the electron donating & withdrawing groups (EDGs)& (EWGs), and nature of the chemical bonds [25]–[27]. Increasing the longitudinal conjugated system leads to increase the electron density pathway of delocalized electrons in the backbone structure which directly influence the nonlinear optical response performance of the molecule [28]. Planarity of the molecular structure affects the NLO response in terms of the ease in transfer of intramolecular charge (ICT). This planarity can be described with the help of dihedral angles between the compound's moieties planes [29], [30]. The strength of ICT within the molecule which directly influence the optoelectronic behaviour of the materials depends on the presence and strength of the EDG and EWG substituents. Besides the electronic properties, organic NLO depend on the degree of charge separation i.e. polarizability and hyperpolarizability phenomena [31].

1.4 Problem statement

Nonlinear optical (NLO) materials have gained attention in recent years due to their outstanding potentiality in integrated NLO photonics from laser frequency conversion to optical communications. However, the development of new synthesized structure with new concepts is ongoing due to the limitations of currently available NLO materials. Over the past few decades, researchers have made affordable efforts to explore the optical nonlinearity response of inorganic materials such as potassium dihydrogen phosphate (KDP) and its derivatives due to their excellent NLO properties, high mechanical stability, and high melting point [7]. However, there are several limitations to the use of the inorganic materials as NLO materials including

limited transparency in visible light, high dielectric constant, limited tunability for specific applications, high cost, and low thermal stability [32], [33]. To overcome these issues, the NLO organic materials such as polymers and dendrimers have been proposed. Polymers are excellent materials in enhancing NLO response since they possess very strong electron donor/acceptor groups and large conjugated system, however the low NLO efficiency and poor thermal stability limit their use as NLO materials [32].

Recently, significant attention has been given to the synthesis organic NLO materials due to several advantages, including ease of synthesis, optical transparency over most visible region, and good crystallizability. Among these materials, chalcone derivatives have grabbed the interest in this field due to their strong delocalized π-electron system, cost-effective synthesis with high yields, and the structural flexibility they offer. This flexibility allows the design of push-pull π-conjugated frameworks by incorporating EDG and EWG at their terminals, which provides tunability in polarizability response [28], [34]. However, despite the potential of strong electron-donating pyrene groups within chalcone-based push-pull systems as promising organic NLO materials, studies focusing on both their electronic and molecular characterizations are limited.

Additionally, there is prevailing need to investigate NLO properties for this kind of materials, particularly in response to the continuous-wave (CW) laser beam, which is important in practical optoelectronic devices and medical applications. In medicine, CW lasers are extensively used for both treatment and diagnostic purposes, such as soft tissue applications in urology [35] and cancer cell photothermal therapy [36]. Various potential optoelectronic applications also employ CW laser, including network analysis [37] and THz photmixing systems [38]. However, most of previous

studies focus on pulsed laser response to study the NLO effect leaving a gap in understanding the behaviour of these materials under CW laser. Furthermore, the relationship between the molecular structure and NLO response under CW laser is still not completed explored [39].

1.5 Objectives

The aims of the study are:

1. To synthesize and characterize a new organic series of pyrenyl-chalcones (PChs) derivatives with various substituents, including halogens, amines, thiophenes, and hydrocarbons.
2. To investigate the correlation between molecular structure, including the effects of EDGs and EWGs, and the physical and optical properties of these PChs derivatives using both experimental and computational methods.
3. To study the potential of synthesized PChs as NLO and OL materials under CW laser beam.

CHAPTER 2

LITERATURE REVIEW

Chalcones are a class of organic materials consisting of two aromatic rings connected by an enone linker, exhibiting a wide range of optoelectronic properties. In particular, pyrene-based chalcones feature an extended conjugation system with a high density of delocalized electrons, which significantly enhances their optical and electronic characteristics. Consequently, pyrenyl-chalcones display a strong nonlinear optical (NLO) response.

2.1 Synthesis of chalcones

Several reports were published in synthesizing chalcones such as Suzuki coupling reaction, Wittig reaction, microwave-assisted reactions, and Claisen-Schmidt techniques[40]–[43]. Among them Claisen-Schmidt condensation, which is selected as a synthesis method in this study, is considered as one of the most reliable approaches due to their simplicity and highly amount of yield can be collected [41]. In this method, the condensation between aryl ketones and aromatic aldehydes in basic/acidic polar solvent media forms connected link of the two aromatic rings via a three carbon-α, β-unsaturated carbonyl system as shown in Figure 2.1.

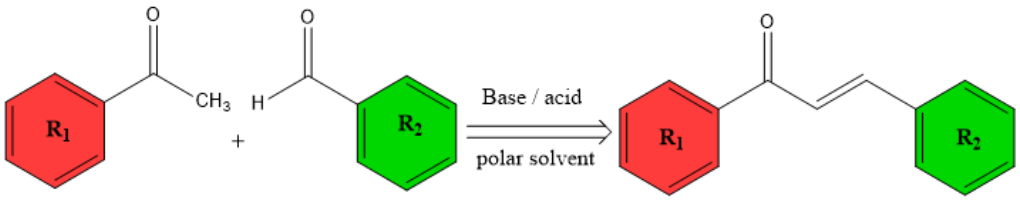

Figure 2.1 Scheme of Claisen-Schmidt chalcone synthesis method

Table 2.1 summarizes some literature review of Claisen-Schmidt reactions with different catalysts, solvent, reaction time and yield of chalcone derivatives.

Table 2.1 Claisen-Schmidt reaction for some chalcone derivatives

Chalcone derivatives	Catalyst	Solvent	Reaction time (hr)	Yield (%)	Ref.
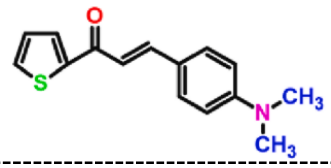	10% NaOH (5mL)	Ethanol	3-4	88	[44]
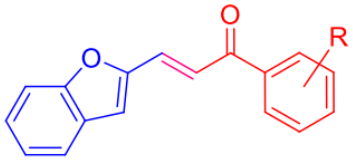	4% KOH	Ethanol	2-3	70	[45]
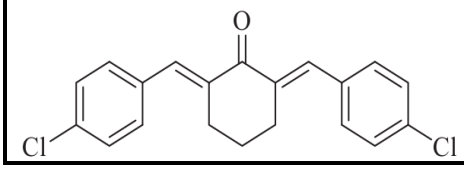	10% LiOH	H_2O	3	87	[46]

2.2 Single crystal XRD structural studies

The crystallographic configurations of chalcones play a significant factor in optical properties in terms of linear and nonlinear effects such as electronic transition, revers saturable absorption (RSA), and two photon absorption (TPA) [47], [48] . Zhang et al. (2016) studied the influence of configurational isomerism on fluorescent characteristics of some chalcone derivatives. In this study, it is reported that the optical properties differ from molecule to another related to two factors: configuration either s-cis or s-trans with respect to central C=C bond, and the arrangement of the molecules within bulk solid. In s-cis conformation, the two aromatic rings at the edge are in same plane, while in s-trans the two aromatic rings are in different planes as shown in Figure 2.2. This arrangement includes monomer arrangement, edge-to-face π- π stacking, and face-to-face π- π stacking. Additionally, it is concluded that the pyrene and anthracene moieties exhibit large red-shifted emissions due to presence of π-stacked geomery [21].

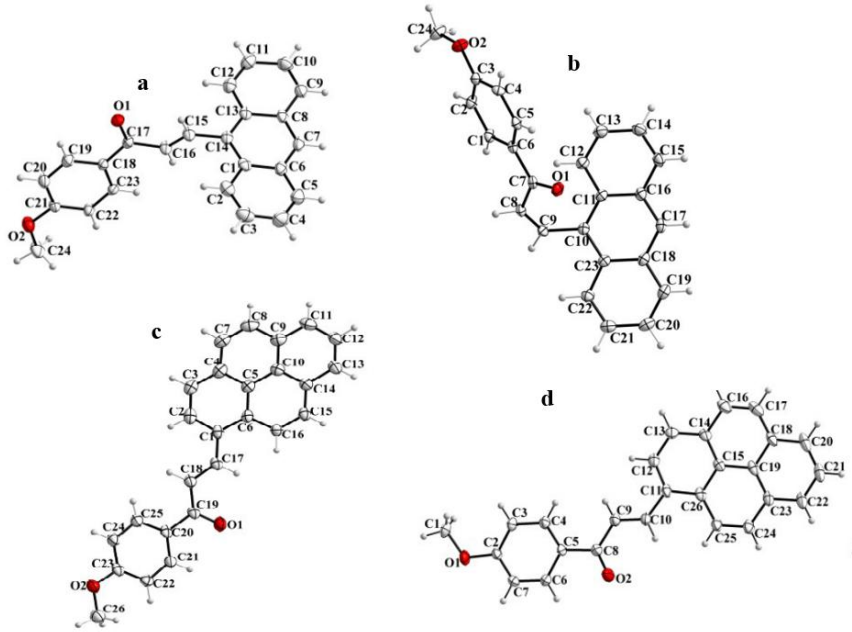

Figure 2.2 Different types of crystal configuration of anthracene in a) *s-trans* b) *s-cis* and pyrene in c) *s-trans* d) *s-cis* configurations, respectively [21]

Molecular geometry is one of the most significant factors on intramolecular charge transfer (ICT) mechanism i.e., the optical and electronic behaviour of the organic compound. Planarity of the molecule affect both ICT strength and conjugation of overall molecule [49]. Zainuri *et al.* (2018) reported that the interactions between anthracene and the enone bridge in anthracene based chalcones are highly influenced by the dihedral angle between these parts i.e. large dihedral close to 90° hinder the interactions [50] as depicted in Figure 2.3.

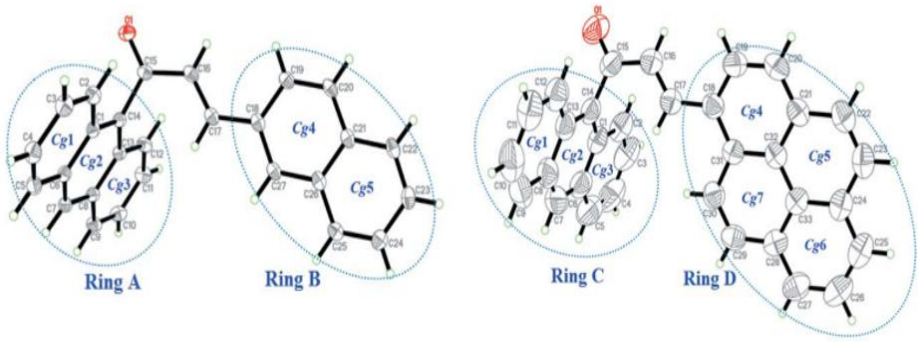

Figure 2.3 The ORTEP diagram of two anthracene based chalcones, shows the high value of dihedral angle between the anthracene and enone linkage which could impede the charge transfer within molecule [50]

In a study conducted by Nizar *et al.* (2023), The planarity backbone of PyBr compound (Figure 2.4) improves the ICT which is obviously enhance the performance of the prepared DSSC compared to the twisted structure of PyF [51]. However, In NLO performance the twisted structure could enhance the nonlinearity optical behavior due to the increasing in polarization of twisted system compared to planarity geometries. According to Lou and his group, twisted π-system (Figure 2.5) can stimulate twisted intramolecular charge transfer (TICT) which dramatically contribute to the NLO response of the compound [10].

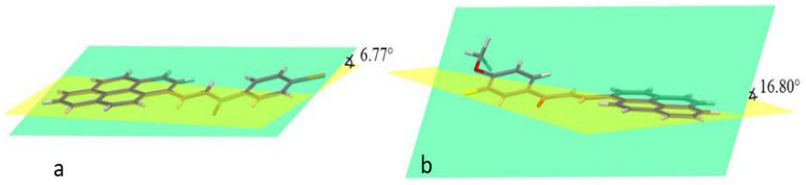

Figure 2.4 Dihedral angle between pyrene and a) 4′-bromoacetophenone (PyBr) and b) 3′-fluoro-4′- methoxyacetophenone (PyF) show the planarity of overall molecules [51]

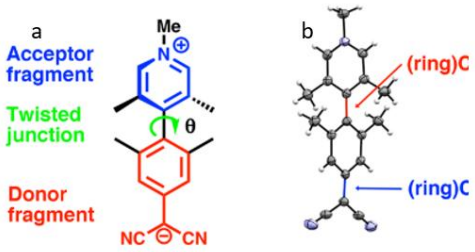

Figure 2.5 a) Typical TICT chromophore with a sterically enforced biaryl torsional angle, θ b) ORTEP image of the molecular structure (30% ellipsoids) of TMC-1[10]

It is reported that in organic materials, different weak intermolecular interactions such as hydrogen bonds, halogen bonds, and π-π stacking interactions have a major contribution on extension crystal pattern [52]–[54]. These kind of interactions are responsible for the crystal configuration to connect the molecules of the compound in head to tail, face-to-face, head-to-head fashions [55]. In pyrene based chalcones, different types of fashion arrangement are reported including head-to-tail (C-H···O) [2], edge-to-face [56], and face-to-face (π…π) [57] arrangements as shown in Figures 2.6, 2.7, and 2.8, respectively.

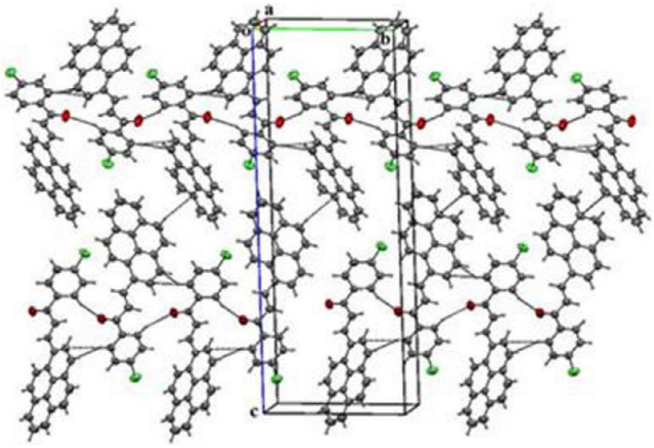

Figure 2.6 Crystal packing for PCP crystal shows head to tail configuration [2]

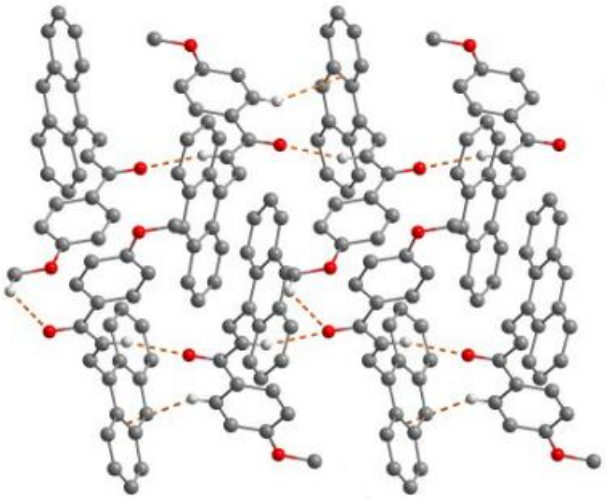

Figure 2.8 Crystal packing for pyrenyl chalcone crystal shows edge-to-face configuration slipped π…π interactions [56]

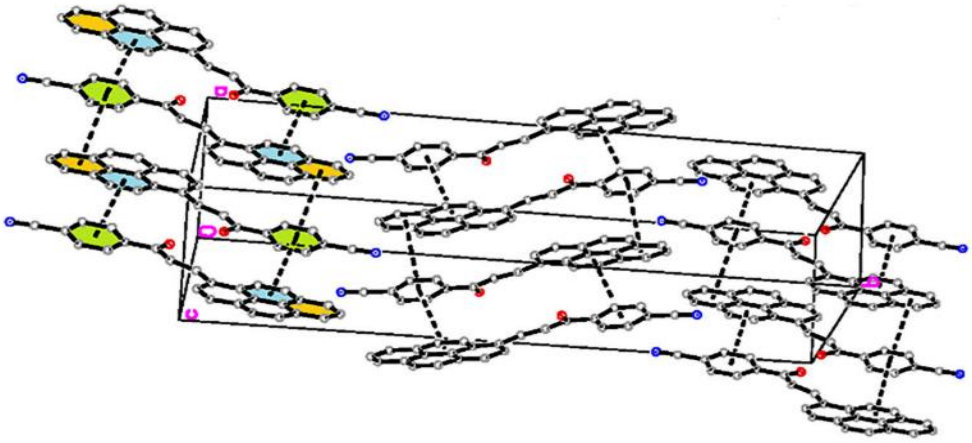

Figure 2.7 Crystal packing for pyrenyl-chalcone crystal shows face-to-face fashion due to π…π interactions [57]

2.3 Optical and electronic transition on chalcones

Ultraviolet-Visible (UV-Vis) spectroscopy is a simple and effective technique for studying optical and electronic transition in organic materials. The UV-Vis absorption spectra arise from the electronic transitions from one electronic state to another, revealing important information about molecular optoelectronic transitions. Additionally, this spectrum indicates the operational wavelength range for optical nonlinearity. For example, high absorption in the UV region and high transparency in the visible range suggest strong potential for use as NLO materials [58], [59].

In chalcones, UV-Vis absorption spectrum consists of two essential absorption bands band I and band II originated from $n \rightarrow \pi^*$ and $\pi \rightarrow \pi^*$ transitions, respectively [60], [61]. In $n \rightarrow \pi^*$ electronic transition, the nonbonding electrons which initially exist in n-orbital absorb the radiation and excite to the higher-energy antibonding π^*-orbital i.e., from HOMO to LUMO orbitals [24]. The $n \rightarrow \pi^*$ transitions appear owing to presence of C=O, aromatic rings, and delocalized electrons in a range close to visible range [320-390nm] which could extend to higher wavelengths. While the delocalized π-electrons in double bond and aromatic rings enable to excite from the π-bonding orbital to an empty π^*-antibonding orbital making $\pi \rightarrow \pi^*$ transition in UV region within the range of [220-270nm] [62], [63].

Substituents impact on these bands either in shift of the peaks or intensity of absorption light. In a study conducted by Lu and colleagues 2023 (Figure 2.9), it is found that the eight titled chalcones show varying spectrum absorptions in terms of maximum absorption peaks positions depends on the chalcone substituents. In this study, effects of two different variations chalcone structures were investigated on their photophysical and photochemical properties. The first group was designed by fixing the aldehyde precursor and vary the substituents at para positions of the ketones part with four substituents: $N(CH_3)_2$, OCH_3, SCH_3, and F. However, the other part of this study was conducted by fixing the ketone precursor and vary the substituent of the aldehyde part with same previous groups. The findings of the study suggests that the ability of EDGs is the main factor in shifting the absorption peak at band I towards the visible range. For instance, compound C4N presents maximum peak wavelength at 407 nm while for chalcone C4F the maximum absorption peak wavelength is at 306 nm due to the different electronegativity strength of the $N(CH_3)_2$ and F at the same positions in the chalcone structures for the two compounds, respectively. In addition, the more

significant impact on the photophysical properties was observed when the substituents vary at aldehyde side [64].

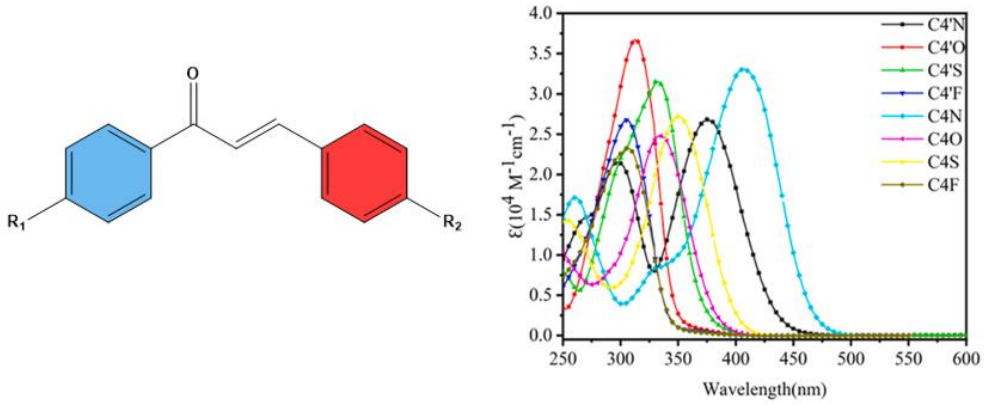

Figure 2.9 Schematic structure of compounds with different substituents and UV-Vis absorption spectra of the chalcone derivatives which show redshift related to strength and position of EDGs [64]

The results of the study conducted by Vasant et al. (2020) suggest that the noticeable difference in optical energy gaps of 3F5B2S (4.7eV) and 4M5B2SC (4.2 eV) compounds is due to the position of fluorine and methoxy functional groups [65]. The fluorine group effect on the compound's structure as an EWG which reduce electron density in the HOMO orbital leading to rise on energy gap of the molecule. On the other hand, methoxy group has an EDG effect which increase electron density on HOMO orbital which shrinks the energy gap. On other interesting study conducted by same group Vasant et al. (2020), it is reported that the energy gap of two halogenated thiophene chalcones are 3.38eV (**B3B2SC**) and 4.43 eV (**C3B2SC**). The molecular structure of these molecules is same with different at para positions of benzaldehyde as shown in Figure 2.10. The findings of this study support the previous discussion of the relation between strength of the functional groups in terms of donating and withdrawing electrons. The **B3B2SC** compound composes of bromine at para position of benzene while **C3B2SC** contains chlorine at the same position. In this case, both chlorine and bromine considered as EWGs however, chlorine has more electronegativity i.e., it has

more electron-withdrawing effect compared to bromine. This is the reason behind the higher value of energy gap of **C3B2SC** (3.43 eV) than **B3B2SC** (3.38eV) [66].

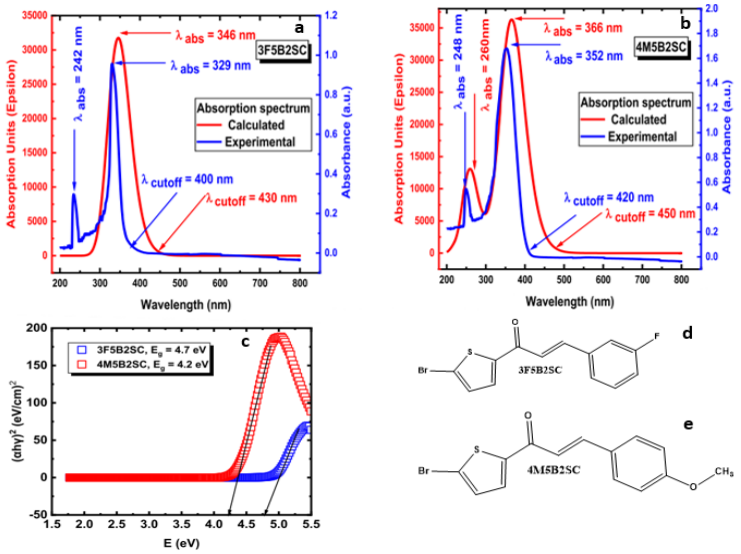

Figure 2.10 Experimental and calculated UV-Vis absorption spectra of a) 3F5B2SC b) 4M5B2SC, C) Tauc's plot of 3F5B2SC and 4M5B2SC, Scheme structure of d) 3F5B2SC e) 4M5B2SC [65]

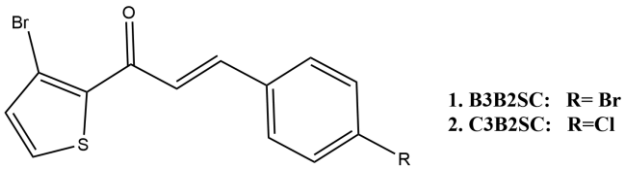

Figure 2.11 Scheme structure of B3B2SC and C3B2SC chalcones [66]

Le et al. (2023) have reported the effect of solvent polarity on the photophysical properties of chalcone compound named (E)-3-(4-(dimethylamino)phenyl)-1-(4-ethoxyphenyl)prop-2-en-1-one (compound **1**). It is observed positive solvatochromism causing a redshift of the maximum wavelength in both absorption bands I and II (Figure 2.12) with increasing solvent polarity [67]. This impact is highly pronounced in the case of longer π-conjugated compound **2** owing to behavior of ICT of Franck-Condon exited state. On the same study, the impact of extension π-conjugation system on the absorption peaks, it is found that extension the π-conjugated system of the compound

leads to redshift due to an increase on π-delocalised electrons [67]. On another study conducted by Irfan et al. (2023), it is observed that no effect of solvent polarity on the electronic transition i.e., energy gap of the compound under different solvent environment are same [68]. However, this study is a computational investigation. Thus, the solvent environment affects the interaction between the molecules of the compound, rather than altering the structure of the compound itself. The intermolecular interactions in this case cannot be observed on computational study.

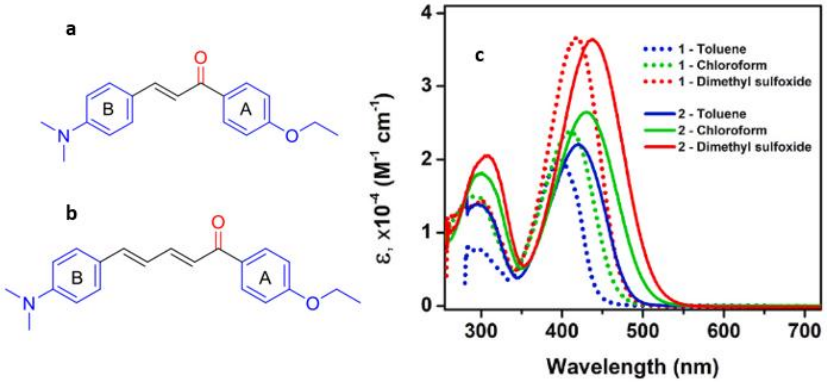

Figure 2.12 Schematic structure of compounds a) 1 b) 2 and c) UV-Vis absorption spectra which show positive solvatochromism in both cases; increasing solvent polarity and extend π-conjugation system dots (compound 1) and lines (compound 2) [67]

2.4 Third order NLO

The nonlinearity effects on organic materials were passionately investigated to understand the mechanism of NLO phenomena. The main cause of NLO phenomena is the polarization of the material, however many factors play significant roles on this polarization. Till today, the studied factors are under debate and precise underlying details are not fully understood. However, several factors have been investigated to explain NLO effects, such as two photon absorption [69], π-delocalised electrons [31], intramolecular charge transfer (ICT) [31], twisted intramolecular charge transfer (TICT) [10], conformational planarization [70], and molecular arrangement [71].

Abu Bakar et al. (2023) have studied the effect of the laser wavelength on profile of the NLO [72]. They claimed that the nonlinearity cause is due to non-degenerate two-photon absorption (TPA) effect in which the photon input energy ($h\nu$) follow the condition of $E_g/2 < h\nu < E_g$ where E_g is the sample energy gap. The effect of the laser power causes the reversal of n_2 polarity which can be shown in the NLR profiles as presented in Figure 2.13. The findings revealed that the sign of the n_2 is reversed at short wavelength of 420 nm compared to other wavelengths of 637 nm and 800nm. At 637nm and 800nm the profiles form valley followed by peak related to the positive n_2 due to the self-focusing. However, the self-defocusing effect at 420nm change the NLR profile to have negative n_2 [72].

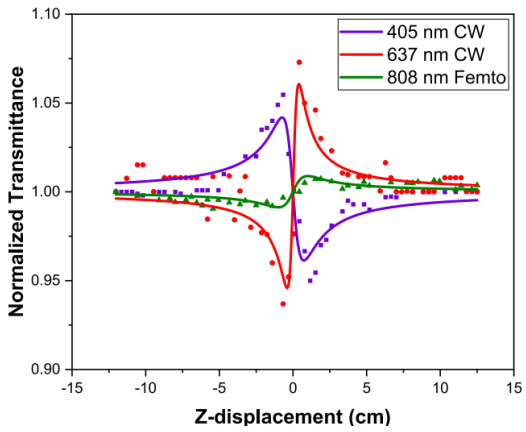

Figure 2.13 NLR profiles of the prepared GaN thin films at CW laser wavelengths of 405nm, 637nm, and pulse laser at 800nm [72].

Shetty et al. (2016) studied the impact of laser input irradiance on the effective nonlinear absorption (NLA) coefficient (β_{eff}) of studied chalcone compound. The findings of this study show that the NLA is caused by reverse saturable absorption

(RSA) and there is an inverse relationship between β_{eff} and laser input irradiance as shown in Figure 2.14 [58].

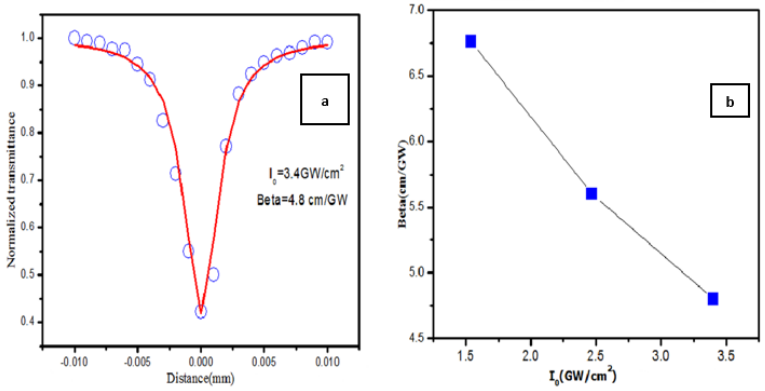

Figure 2.14 a) NLA profile at I_o=3.4GW/cm^2 and b) NLA coefficient as a function of input irradiance

The effects of molecular structure of the compounds on NLO properties of four halogenated chalcone derivatives was investigated by Wong et al (2022). In this study [27], It is reported that the intermolecular interactions of compound play a role on NLO of the compound. Due to this, compound III which have higher intermolecular interactions shows the highest NLO responses among the three studied halogenated chalcone compounds. Similar findings reported by Maidur et al. (2021) who have studied the ultrafast NLO of two pyridine-based anthracene called **2PANC** and **3PANC** under 50 fs and 800 nm pulsed laser and obtained NLO results [24]. It is reported that the RSA due to TPA is the reason behind the nonlinear absorption (NLA) phenomena. The two compounds present high NLO response; however, 2PANC shows higher NLO response than 3PANC due to presence of intermolecular interaction of C−H···N−C in 2PANC and absent of this kind of interaction in 3PANC. Shaty et al. (2017) conducted a similar study in investigating the effect of molecular structure of D−A − π − D

(**FMOC-3**) and D−A − π − A(**FMOC-7**) on NLO response [73]. It is reported that molecular structure of both FMOC compounds (Figure 2.15) contribute to NLO response of the molecules. The two EDGs at para positions of the ends in FMOC-3 gives rise to charge transfer towards the acceptor part at center of the molecule C=O group. In the FMOC-7 case, chlorine group at the end of the chalcone provides strong acceptor group which increases the charge transfer within D−A − π − A configuration structure. Consequently the direction of charge transfer towards the end part of the molecule as a result the NLO response is higher in FMOC-7 compound compared to FMOC-3 [73].

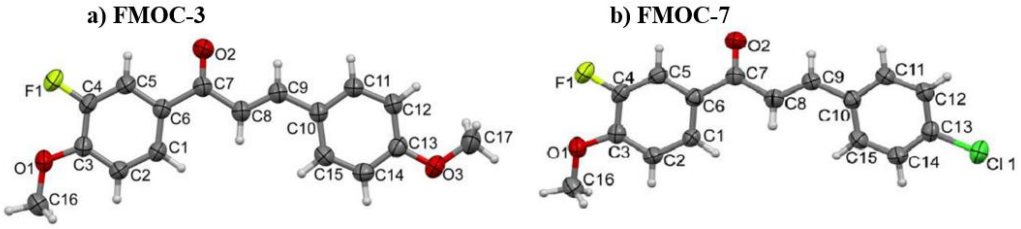

Figure 2.15 ORTEP diagram of molecular structure of a) FMOC-3 and b) FMOC-7 [73]

From the literature survey (Table 2.2), the chalcone derivatives show high value of NLO properties with different range of response related to the factors which are explained above [57], [74]–[76]. On the study conducted by Sun et al. (2019), it is reported that the minimum steric hindrance on the compound **3b** gives higher strong on the conjugated system. As a result, delocalized π-electrons can be polarized easier than other compounds **3a**, **3c**, and **3d** as presented in Table 2.2 [74]. In view of ICT, the distortion of π-conjugated system influence NLO response of organic compounds [74]. The study conducted by Zainuri et al. 2023 investigated the response of two chalcones under CW laser, it is reported that the compound AP (pyreneyl-chalcone) exhibits higher $\chi^{(3)}$ compared to AT (anthracenyl-chalcone) due to the higher π-conjugated

system of the pyrene compared to anthracene [57]. Table 2.2 represent some chalcones response to NLO effect under high intensive laser beam.

Table 2.2 Third order NLO properties of different chalcone derivatives

Molecule		Laser properties	β 10^{-9} cm/W	n_2 10^{-13} cm^2/W	$\chi^{(3)}$ 10^{-12} esu	Ref.
AP	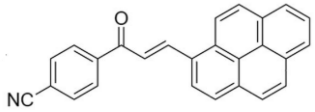	CW 637nm 1.6kW/cm^2	3.8E5	3.47E5	5.2E5	[57]
3a	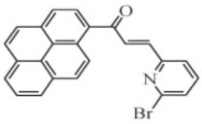	Pulsed 460 nm $t\sim4ns$	170	7.8	54.9	[74]
3b	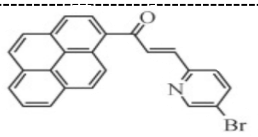		205	15.7	96.1	
3c	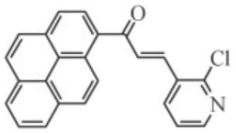		31	6.2	35	
3d	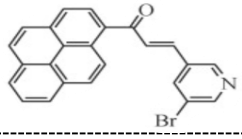		49	0.9	11.1	
CPDAPP	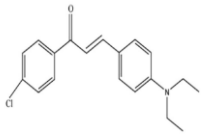	CW 532 nm 200mW	11.2E5	1.25E5	7.12E5	[75]
DA-ANC	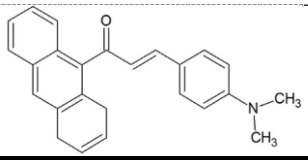	CW 532 nm 200 mW	6.9E4	1.31E5	7.49E5	[76]

2.5 Computational studies

Density Functional theory (DFT) is one of the most effective theories to investigate the electronic structure of atoms, molecules, and compounds. Unlike traditional electronic structure approach, in which the solution of Schrodinger equation for N electrons is a complicated many-body wave function, the DFT which is found by

Hohenberg-Kohn and Kohn-Sham theorems deals with system as one-body density with solution of density n(r) as a function of spatial coordinates. To improve the accuracy for this theory and to be helpful for the practical computations, approximation for the exchange correlation called functional is suggested. The functional is a mathematical expression to provide approximation of the exchange-correlation energy of the system. The accuracy of the approximations changes from one system to another related to suitable approximations comes from the utilized functional. One of the most effective hybrids functional used in organic materials is Becke's three-parameter with the Lee-Yang-Parr correlation functional (B3LYP). In B3LYP, the exchange correlation contains Hartree-Fock exchange, local density approximation (LDA), and generalized gradient approximation (GGA) [77]–[79].

In order to represent the electron density of the system n(r), number of mathematical functions called basis set can be used, this representation provides clear information about the molecular orbitals which are optimized to extract the chemical properties of the studied system. Basis sets come in several sizes and levels of sophistications in terms of number of functions in these basis sets. The 6-311++G(d,p), which is used in this study, is a valance triple zeta (VTZ) basis set with following information of the built basis function: 6 primitive Gaussian functions for each core orbitals, 3 primitivities for inner valance, and a single uncontracted primitive for the outer valance with polarization function. The first (+) sign indicates that diffuse s-and p-functions are added to heavy atoms and the second (+) sign corresponding to a set of diffuse s-functions added to each hydrogen atom. (d,p) indicates the polarizing d-function of heavy atoms and p-function for hydrogen atom. Recently, computational studies have emerged as a powerful approach for investigating molecular structure and understanding how structural backbone and its derivatives influence optoelectronic

properties. In conducting this investigation, the initial step involves optimizing the geometric structure of the compound. Extensive efforts have been focused on choosing the effective theories for optimizing chalcone derivatives. Among them, DFT with the B3LYP functional and the 6-311++G(d,p) basis set has proven highly accurate in determining molecular geometries with high level of reliability compared to experimental data [80]–[83]. However, disparities between the optimized and experimental geometries can arise due to the presence of hydrogen bond interactions of neighbouring molecules i.e., quantum computations are typically performed for only individual molecule [84].

Kumar et al. (2014) performed experimental and computational study on molecular structure of a single crystal based on chalcone configuration named as (2E)-1-(5-chlorothiophen-2-yl)-3-(naphthalen-2-yl) prop-2-en-1-one as shown in Figure 2.15 [85]. In their computational work, they used DFT theory with B3LYP functional at 6-311+G(3df,p) basis set (Figure 2.16). The authors found that the largest variance observed between the XRD data and computational of the bond length, angles degree, and torsional are 0.157 Å, 2.5°, and 7.5°, respectively. Furthormor, the corelations R^2 between the experimental and DFT calculations were found to be (0.9774, 0.9737, and 0.9997) for the *s-trans*, and (0.9784,0.8046, and 0.94) for the *s-cis* configurations of the bond lengths, angles, and torsional angles, respectively [85]. The high agreement between the experimental and calculated geometries shows that the B3LYP functional is one of the most significant functional suitable for the chalcone derivatives.

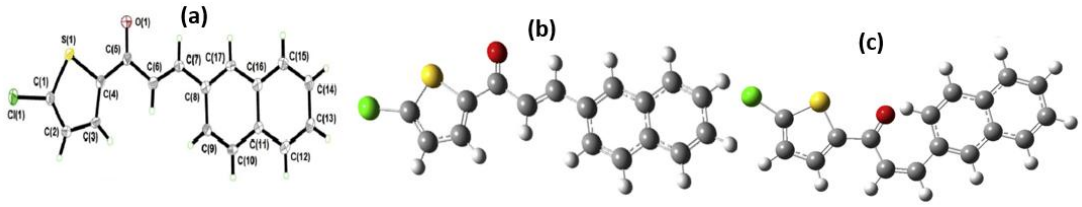

Figure 2.16 a) Molecular view of ORTEP diagram with atomic labelling @ 50% probability displacement ellipsoid, optimized structure b) *s-trans*, and c) *s-cis* isomers of the studied compound [85].

On another study conducted by Wong et al. (2022) on effect of the substitutional position of two thienyl based chalcones on photophysical and NLO properties using both computational and experimental investigation [86]. The computational studies were utilized using DFT theory with B3LYP functional and 6-311++G(d,p) basis set. The findings of this study show that there is well agreement between the calculations and experimental of both bond lengths and dihedral angles as shown in Figure 2.17. However, there is considerable deviation on the torsion angles [86]. This deviation could be due the impact of the crystal packing which cannot be investigated by computational analysis.

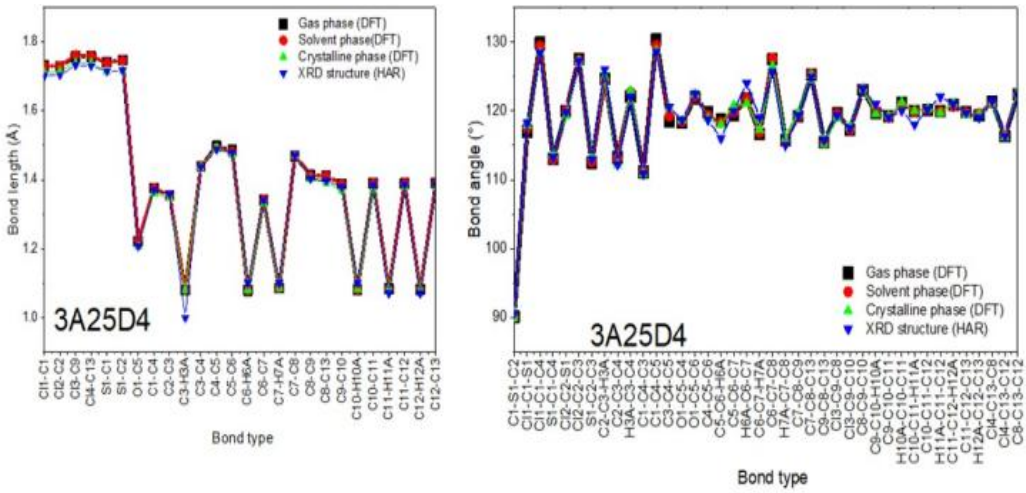

Figure 2.17 Bond length and bond angle variations for the optimized and Hirshfeld atom refinement (HAR-XRD) structure of the 3A25D4 titled compound [86].